energies

Article

A Bi-Directional Dual-Input Dual-Output Converter for Voltage Balancer in Bipolar DC Microgrid

Sung-Hun Kim, Hyung-Jun Byun, Junsin Yi and Chung-Yuen Won *

Department of Electrical and Computer Engineering, College of Information and Communication Engineering, Sungkyunkwan University, Suwon 16419, Korea; regar14@skku.edu (S.-H.K.); gudwns313@skku.edu (H.-J.B.); junsin@skku.edu (J.Y.)
* Correspondence: woncy@skku.edu

Abstract: Bipolar DC microgrids (BDCMGs) have several issues related to the voltage and require numerous converters to supply power to both poles. To solve these issues, a bidirectional dual-input dual-output (DIDO) converter is proposed for the voltage balancer in BDCMG. The DIDO converter has dual-input sources and a dual-output port connected to the grid. Additionally, the DIDO converter simultaneously performs independent bidirectional power control and voltage balancing control. Based on the input voltages, this paper proposes modulation methods for three cases. The modulation method of the second case has a wide operating range and low balancing current ripple without increasing the switching frequency. Moreover, only voltage balancer mode without active input sources is proposed, considering the intermittent source. Therefore, it can operate as a voltage balancer under all conditions. The voltage balancing performance of the three cases was analyzed. Finally, the proposed modulation and control method of the DIDO converter were verified through experimental results.

Keywords: bipolar DC microgrid; dual-input dual-output converter; bidirectional converter; voltage balancer

Citation: Kim, S.-H.; Byun, H.-J.; Yi, J.; Won, C.-Y. A Bi-Directional Dual-Input Dual-Output Converter for Voltage Balancer in Bipolar DC Microgrid. *Energies* **2022**, *15*, 5043. https://doi.org/10.3390/en15145043

Academic Editor: Panos Kotsampopoulos

Received: 23 May 2022
Accepted: 28 June 2022
Published: 11 July 2022

1. Introduction

Renewable energy sources such as photovoltaics (PV) and wind energy are used extensively, and microgrids (MGs) are an important research area in this regard. MGs are classified as AC and DC MG. In particular, the DC MG reduces power conversion losses and has simple control structures, because DC MGs do not have reactive power and synchronization issues [1–5].

DC MGs are classified into two types: unipolar and bipolar. In particular, bipolar DC microgrids (BDCMGs) use two voltage levels with three wires, as shown in Figure 1. Further, a BDCMG has higher reliability than unipolar DC microgrids, because BDCMG can use independent DC buses [6,7]. Grid-connected converters use a suitable voltage level in BDCMG. However, a BDCMG has several problems. The main issue is that a large number of converters are required for positive, negative and DC buses. Additionally, unbalanced voltage occurs depending on the load conditions in the positive and negative buses. The unbalanced voltage causes low reliability and reduces the quality of the BDCMG. Voltage balancers that control the voltage deviation of the bipolar DC bus are commonly used to solve unbalanced voltages in BDCMG [8–10].

To solve the aforementioned main issues, a combined converter with voltage balancer and various converter have been proposed previously [11–20]. A non-isolated SEPIK-Cuk converter combined SEPIC and Cuk converter [11]; however, these converters are unidirectional converters. The dual output boost converter combines two boost converters with independent voltage control loops [12]. A combined boost-SEPIC type interleaved DC–DC converter [13], and a voltage balancer with an EV charger [14], a non-isolated three-level converter for voltage balancer [15,16], and a bi-directional DC–DC boost converter with additional inductors [17] were proposed. These non-isolated conventional converters have a single input source and are used as voltage balancers. Moreover, isolated topologies in BDCMG have been proposed in [18,19]. In [18], a three-level dual active bridge (DAB) converter with a modulation balancing method was introduced. The DAB converter operates without additional passive elements. The DAB converter and interleaved buck-boost converter were combined in [19] as a voltage balancer.

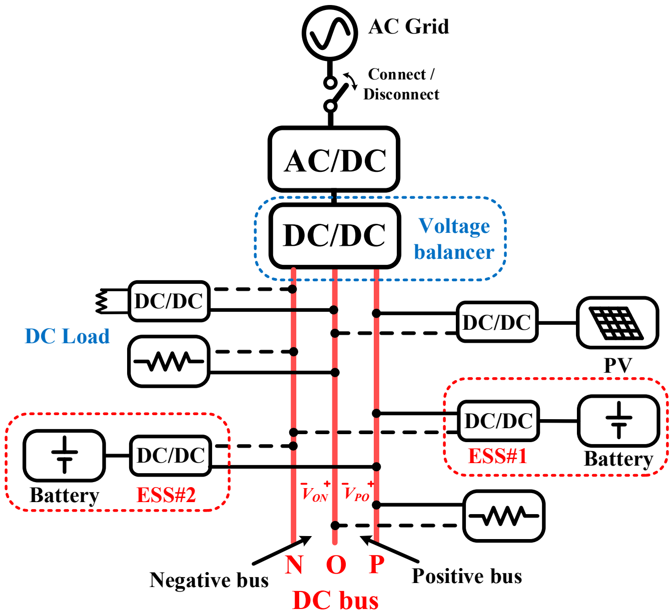

Figure 1. Configuration of the bipolar DC microgrid.

To control voltage balancing, these conventional converters supply power from an input source to the unbalanced load of the bipolar bus with balancing control. Otherwise, balancing control is possible only when power is supplied to the load. However, grid-connected converters of DCMGs use several intermittent sources. As a result, if the input sources are inactive, the operation of the voltage balancer is limited in BDCMG.

The aforementioned study has only a single input source. Moreover, a non-isolated dual-input dual-output (DIDO) unidirectional DC–DC converter for BDCMG was proposed in [20]. This converter controls a dual input source and regulates one of the bipolar bus voltages with one active input source. However, this converter performs unidirectional power flow and has limitations in voltage balancing because it requires an active input source. A comparison of conventional converters and the proposed DIDO converter is presented in Table 1.

Table 1. Comparison of conventional converters and proposed dual-input dual-output converter for BDCMG.

Ref	Topology	Input Sources of Converter	Control and Voltage Balancing Method	Voltage Balancing without Input Source
[11]	SEPIC-Cuk Combination Converter	Single source	Unidirectional control with voltage balancing	No
[12]	Dual Output Boost Converter	Single source	Independent voltage control loops	No
[13]	Boost-SEPIC Interleaved Converter	Single source	Bidirectional control with voltage balancing	Yes

Table 1. *Cont.*

Ref	Topology	Input Sources of Converter	Control and Voltage Balancing Method	Voltage Balancing without Input Source
[14]	Modified Series-capacitor Converter	Single source	Bidirectional control with voltage balancing	No
[15]	Buck three-level Converter	Single source	Balancing control with modulation method	No
[16]	Full-bridge three-level Converter	Single source	Balancing control with modulation method	No
[17]	Integrated three-level Boost Converter	Single source	Independent voltage control loops	Not considered
[18]	Three-level DAB Converter	Single source	Balancing control with modulation method	No
[19]	Enhanced Two-level DAB Converter	Single source	Bidirectional control with voltage balancing	Not considered
[20]	DIDO Unidirectional DC–DC Converter	Dual sources	Unidirectional control with single bus voltage control	No
This paper	DIDO Bidirectional DC–DC Converter	Dual sources	1. Bidirectional and voltage balancing control with modulation method 2. Only voltage balancer mode without input sources	Yes

This paper proposes a combined bidirectional DIDO DC–DC converter that is used as a voltage balancer under all conditions with two input sources. Additionally, three types of modulation methods for voltage balancing in a BDCMG are proposed. The major contributions of this paper are summarized as follows:

(1) The DIDO converter simultaneously performs voltage balancing and bidirectional power controls with dual inputs and outputs. Independent bidirectional power control and balancing control are realized under all load conditions.

(2) Three types of modulation methods are performed. All three modulations can compensate for unbalanced power. Among the three types of modulation methods, the second modulation method reduces the current ripple in the voltage balancer without increasing the switching frequency.

(3) To maintain voltage balancing without active input sources, additional modulation and control methods are required. Unlike conventional converters, this paper proposes a voltage balancer mode without active input sources.

The performances of the bidirectional control and voltage balancing were experimentally verified.

2. Proposed DIDO Converter

2.1. Configuration of the DIDO Converter

Figure 2 shows the bidirectional DIDO DC–DC converter. This converter has six power switches (S_1, S_2, S_3, S_4, S_5 and S_6), three inductors (L_1, L_2 and L_3), and four capacitors (C_{in1}, C_{in2}, C_{out1} and C_{out2}). The output is connected to the BDCMG. P, O, and N are the nodes of the positive bus V_{out1} and negative bus V_{out2}. The boost inductors L_1 and L_2 are connected to each input V_{in1} and V_{in2}. R_1 and R_2 are the equivalent loads of the bipolar bus. C_{in1} and C_{in2} are the input capacitors, C_{out1} and C_{out2} are the output capacitors. i_{L1} and i_{L2} are the inductor currents, and i_{L3} is the balancing current. To perform voltage balancing without active input sources, the balancing inductor L_3 is connected directly to the neutral line of the BDCMG. A theoretical analysis of the inductor currents and capacitors in the DIDO converter is presented in Table 2. First duty ratio is D_1, second duty ratio is D_2 and sampling time is T. The passive elements of each converter are designed based on Table 2 and the balancing inductor L_3 is designed for the modulation methods described in the next section.

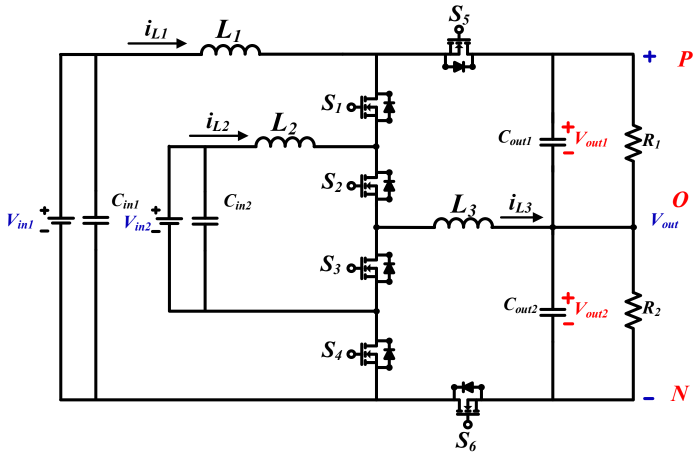

Figure 2. Proposed DIDO DC–DC converter.

Table 2. Theoretical analysis of the DIDO converter.

-	Theoretical Analysis
Δi_{L1}	$\frac{V_{in1} D_1 T}{L_1}$ and $\frac{(V_{in1}-V_{out})(1-D_1)T}{L_1}$
Δi_{L2}	$\frac{V_{in2} D_2 T}{L_2}$ and $\frac{(V_{in2}-V_{out})(1-D_2)T}{L_2}$
Δv_{out}	$\frac{C_{out1} \cdot C_{out2}}{(C_{out1}+C_{out2})}(\frac{V_{out}}{R_1+R_2})D_1 T$
Δv_{in1}	$\frac{1}{L_1 C_{in1}} \frac{V_{out}(1-D_1)D_1 T^2}{8}$
Δv_{in2}	$\frac{1}{L_2 C_{in2}} \frac{V_{out}(1-D_2)D_2 T^2}{8}$

2.2. Modulation Methods of DIDO Converter for Voltage Balancing in BDCMG

To simultaneously control voltage balancing and dual input sources, there are three possible operating cases: A, B and C. Three cases are defined based on d_1 and d_2, and an appropriate modulation method is proposed for each case. In every case, all switches switch only once, and the converter implements independent control loops with the same carrier waveform and switching frequencies.

The first duty ratio d_1 and second duty ratio d_2 have independent voltage gain, expressed as follows:

$$\frac{V_{out}}{V_{in1}} = \frac{1}{(1-d_1)} \tag{1}$$

$$\frac{V_{out}}{V_{in2}} = \frac{1}{(1-d_2)}. \tag{2}$$

The main switches are connected in a series, and the duty ratio d_1 is limited depending on d_2.

$$d_1 \leq d_2. \tag{3}$$

The voltage gain of the voltage balancer is expressed as follows:

$$\frac{V_{out2}}{V_{out1}} = \frac{d_3}{(1-d_3)}. \tag{4}$$

Based on the d_1 and d_2 values, the operating cases are defined as shown in Table 3. Accordingly, Figure 3 shows the typical waveforms of the proposed modulations methods with the voltage balancing method when the equivalent load of the ON bus is a heavy load. In all cases, voltage balancing and bidirectional control are performed simultaneously.

Values d_1 and d_2 are controlled independently; however, d_3 changes depending on the case. In particular, in case B, the balancing current ripple decreases without increasing the number of switching in the main switches.

Table 3. The operating range of duty ratio and used switches for balancing modulations.

Case	Operating Range of Duty Ratio	Used Switches for Voltage Balancing
A	$d_1 \leq d_2 < 0.5$	S_2 or S_3
B	$d_1 < 0.5$ and $d_1 \leq d_2$	S_1, S_2 or S_3, S_4
C	$d_2 - d_1 > 0.5$	S_1 or S_4

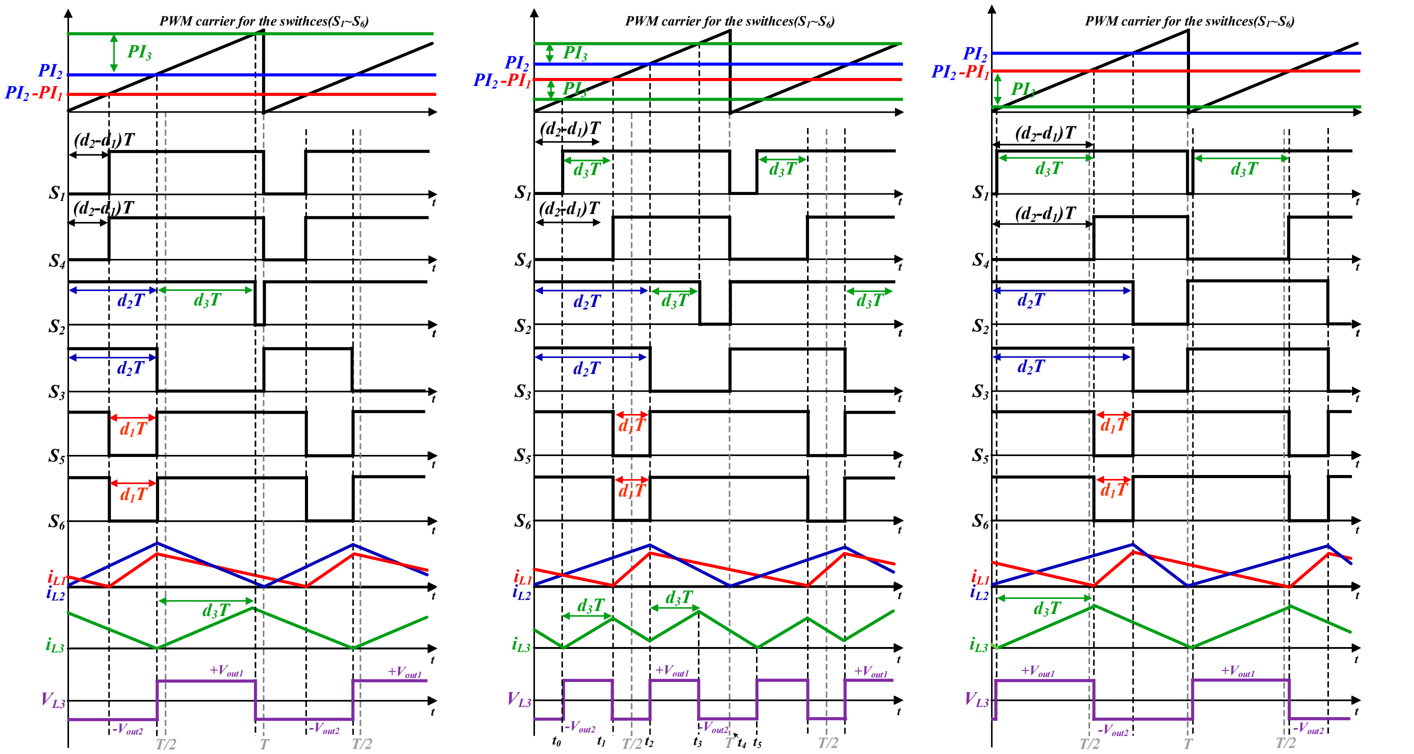

(**a**) (**b**) (**c**)

Figure 3. Typical waveforms of proposed modulation method with voltage balancing methods: (**a**) case A; (**b**) case B; (**c**) case C.

The modulation methods use PI controller. The simple control loops for the grid-connected mode are shown in Figure 4. PI_1 and PI_2 are the outputs of the PI controller in the control loops, and PI_3 is the output of balancing control. Based on the master-slave control of BDCMG, current command references are selected by the master control with communication. To generate the balancing modulation, a flow chart of the balancing modulation is shown in Figure 5. If V_{out1} is larger than V_{out2}, the balancing current is supplied to the ON pole using *Out*1. Conversely, if V_{out2} is larger than V_{out1}, the balancing current is supplied to the PN pole using *Out*2. The modulation methods of the three cases are analyzed below.

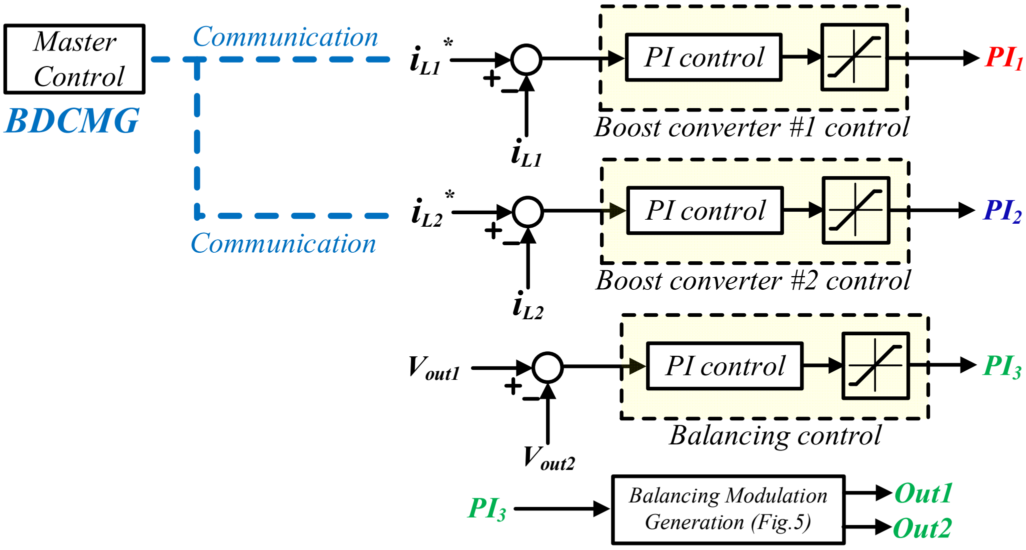

Figure 4. Control block diagram of the bidirectional DIDO converter.

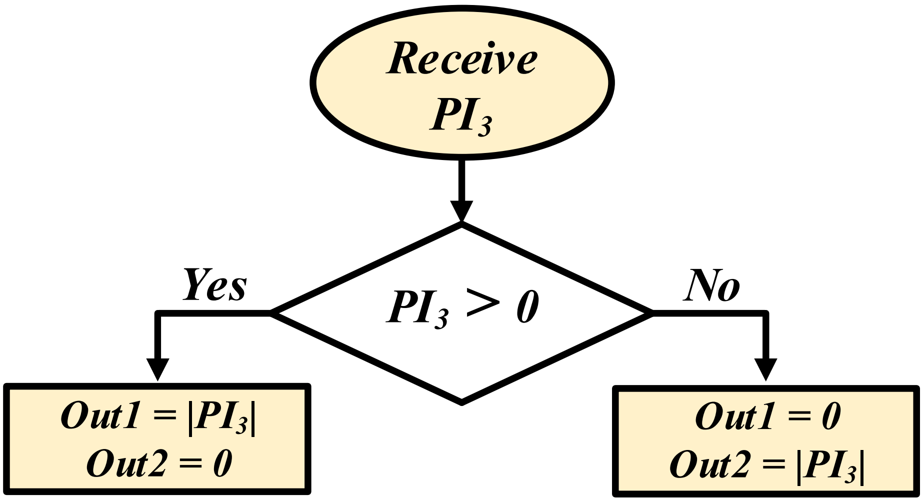

Figure 5. Flow chart of the balancing modulation.

2.2.1. Case A: $d_1 \leq d_2 < 0.5$

Figure 3a shows the typical waveforms of the modulation method in case A. Only one switch (S_2 or S_3) is used for voltage balancing; therefore, the modulation method is simple, as shown in Figure 6. The balancing factors $Out1$ or $Out2$ is added to the PWM reference of the switch (S_2 or S_3) for voltage balancing. If V_{out1} is larger than V_{out2}, $Out1$ is used; alternatively, if V_{out2} is larger than V_{out1}, $Out2$ is used. Consequently, the current ripple of the balancing inductor in the steady-state can be calculated as

$$\Delta i_{L3} = \frac{V_{out1}}{L_3} d_3 T \; or \; \Delta i_{L3} = \frac{-V_{out2}}{L_3}(1 - d_3)T \quad (5)$$

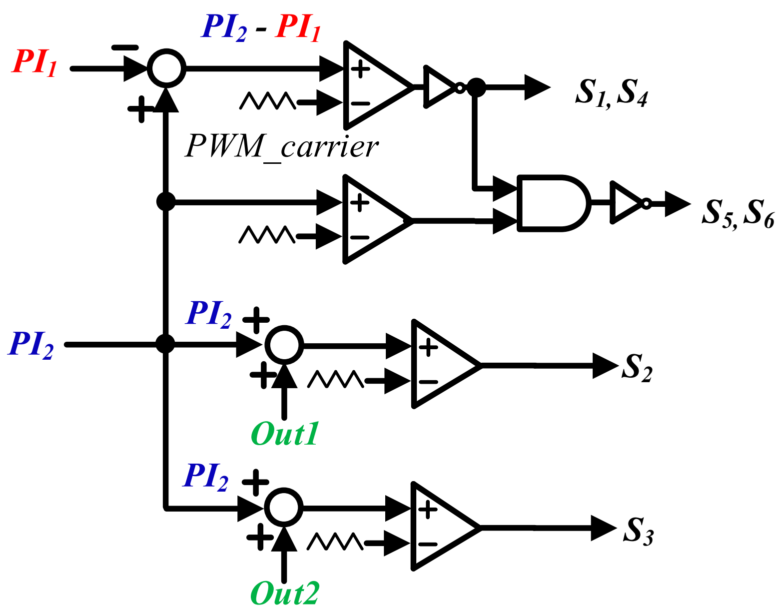

Figure 6. The modulation method of case A.

There is no limit to compensate for unbalanced loads because the balancing inductor is controlled similar to a buck-boost converter.

2.2.2. Case B: $d_1 < 0.5$ and $d_1 \leq d_2$

The second typical waveform of the modulation method in case B is shown in Figure 3b. The modulation method in case B is more complex than those in cases A and C, as shown in Figure 7. However, case B has a wide operation range and lower current ripple, because the voltage of L_3 is supplied twice during one switching period by the switch (S_1, S_2 or S_3, S_4). As a result, the current ripple of L_3 is reduced without increasing the switching frequency. The balancing factors $Out1$ or $Out2$ are added to the PWM reference of a switch (S_2 or S_3) and subtracted from the PWM reference of the other switch (S_1 or S_4). The operating modes in case B are shown in Figure 7.

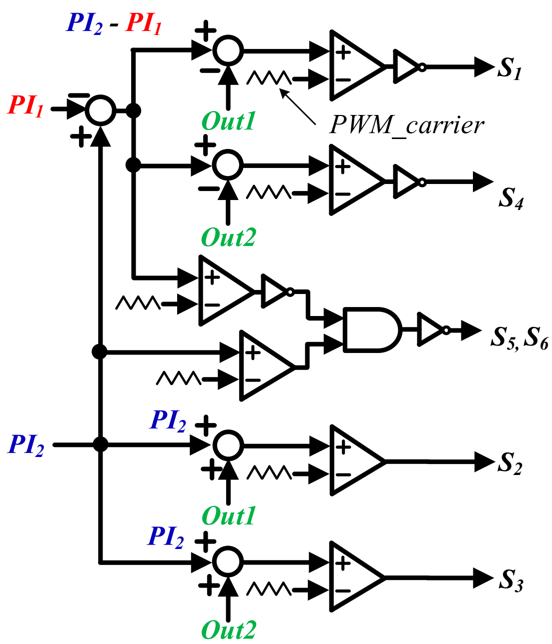

Figure 7. The modulation method of case B.

Mode 1 (t_0–t_1) (Figure 8a): S_1, S_2, S_3, S_5, and S_6 are turned on, and S_4 is turned off. The inductor current i_{L1} is the negative current slope, and i_{L2} is the positive current slope because inductor voltage V_{L1} is V_{in1}–V_{out} and V_{L2} is equal to V_{in2}. The balancing current i_{L3} is the positive current slope generated by V_{out1}.

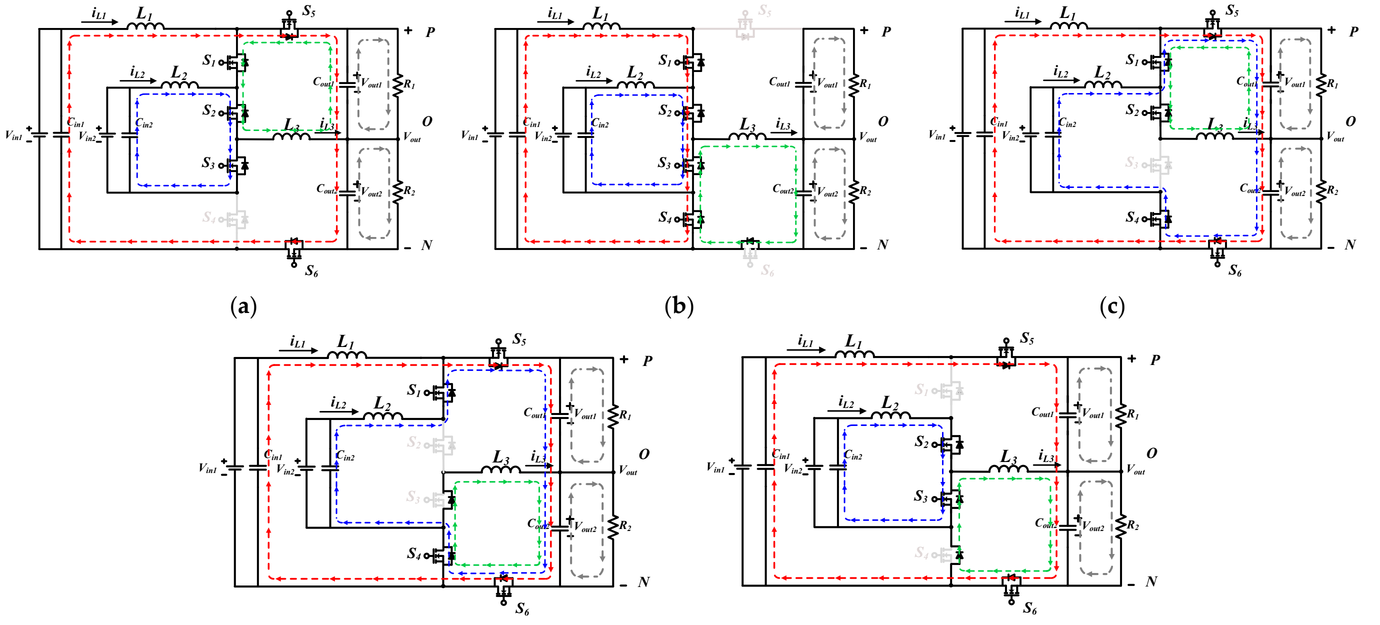

Figure 8. Operating modes of case B: (**a**) mode 1 (t_0–t_1); (**b**) mode 2 (t_1–t_2); (**c**) mode 3 (t_2–t_3); (**d**) mode 4 (t_3–t_4); (**e**) mode 5 (t_4–t_5).

Mode 2 (t_1–t_2) (Figure 8b): S_1, S_2, S_3, and S_4 are turned on, S_5 and S_6 are turned off. All the main switches are turned on. The inductor currents i_{L1} and i_{L2} have a positive current slope because the inductor voltage V_{L1} is V_{in1} and V_{L2} is equal to V_{in2}. The balancing current i_{L3} is the negative current slope generated by $-V_{out2}$. This mode determines the maximum inductor current ripple of L_3.

Mode 3 (t_2–t_3) (Figure 8c): S_1, S_2, S_4, S_5, and S_6 are turned on, and S_3 is turned off. The inductor currents i_{L1} and i_{L2} are negative current slopes because the inductor voltage V_{L1} is V_{in1}–V_{out} and V_{L2} is V_{in2}–V_{out}. The balancing current i_{L3} is the positive current slope once again, like Mode 1. In case B, the current ripple is reduced because this positive current slope is repeated twice.

Mode 4 (t_3–t_4) (Figure 8d): S_1, S_4, S_5, and S_6 are turned on, and S_2, S_3 are turned off. The inductor current i_{L1} and i_{L2} are negative currents as in Mode 3. The balancing current i_{L3} is the negative current slope.

Mode 5 (t_4–t_5) (Figure 8e): S_2, S_4, S_5, and S_6 are turned on, and S_1, S_4 are turned off. The inductor current i_{L1} and i_{L2} are the same as those in mode 1. The balancing current i_{L3} is still the negative current slope. In addition, the maximum current ripple of L_3 changes according to d_1 and d_2. Therefore, an analysis is required for inductor design. The current ripple of L_3 in the steady-state is calculated as follows:

$$\Delta i_{L3} = \begin{cases} \frac{V_{out1}}{L_3} d_3 T & t_0 < t \leq t_1 \\ \frac{-V_{out2}}{L_3} d_1 T & t_1 < t \leq t_2 \\ \frac{V_{out1}}{L_3} d_3 T & t_2 < t \leq t_3 \\ \frac{-V_{out2}}{L_3} (1 - d_1 - 2d_3) T & t_3 < t \leq t_5 \end{cases} \quad (6)$$

Based on Equation (6), the positive current slopes are determined by d_3, but the value of d_3 is equal in the first and third current slopes. Therefore, the maximum current ripple of L_3 is determined by the second and fourth current slope as d_1.

When $d_1 < 0.25$, the maximum current ripple of L_3 is

$$\frac{-V_{out2}}{L_3}d_1T < \frac{-V_{out2}}{L_3}(1-d_1-2d_3)T;\ \text{as } d_1 < 0.25 \tag{7}$$

When $d_1 > 0.25$, the maximum current ripple of L_3 is

$$\frac{-V_{out2}}{L_3}d_1T > \frac{-V_{out2}}{L_3}(1-d_1-2d_3)T;\ \text{as } d_1 > 0.25. \tag{8}$$

Based on Equations (7) and (8), the maximum current ripple of L_3 is calculated based on d_1. When d_1 is 0.25 and V_{PN} is 190 V, the minimum current ripple is half the current ripples of the other cases, as shown in Figure 9.

2.2.3. Case C: $d_2 - d_1 > 0.5$

The modulation method for case C is shown in Figure 3c. Only one switch (S_1 or S_4) is used in the balancing modulation to have a sufficient voltage gain for the balancer. The balancing factors $Out1$ or $Out2$ are subtracted from the PWM reference of the switch (S_1 or S_4) as shown in Figure 10. The modulation method is simple and uses the same voltage gain similar to case A. The current ripples of the buck-boost converter in a steady-state can be calculated as follows:

$$\Delta i_{L3} = \frac{V_{out1}}{L_3}d_3T \text{ or } \Delta i_{L3} = \frac{-V_{out2}}{L_3}(1-d_3)T. \tag{9}$$

The three modulation methods simultaneously perform dual bidirectional power control and voltage balancing control. The duty ratios are independently controlled and voltage balancing is implemented regardless of the unbalanced power.

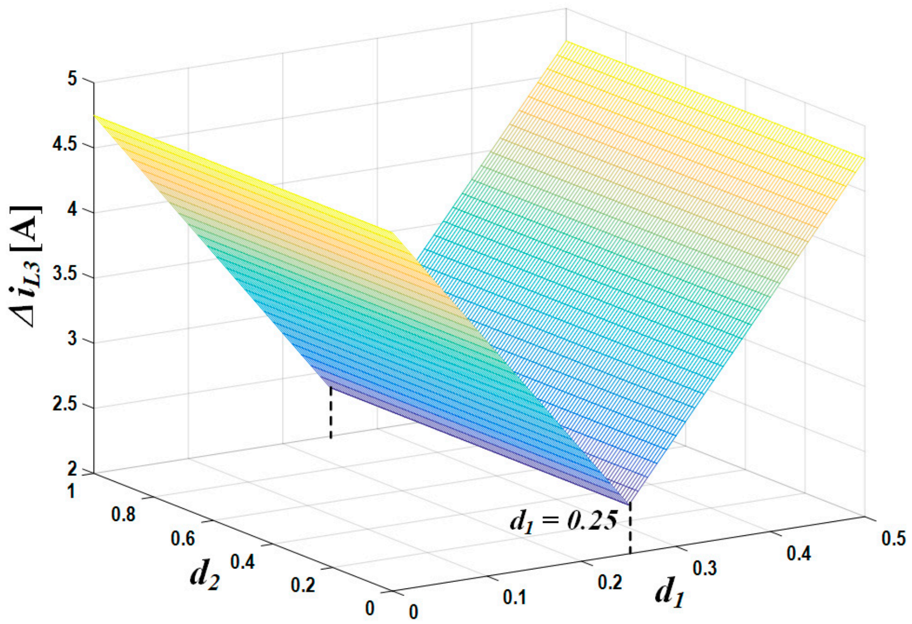

Figure 9. Current ripple of L_3 in case B.

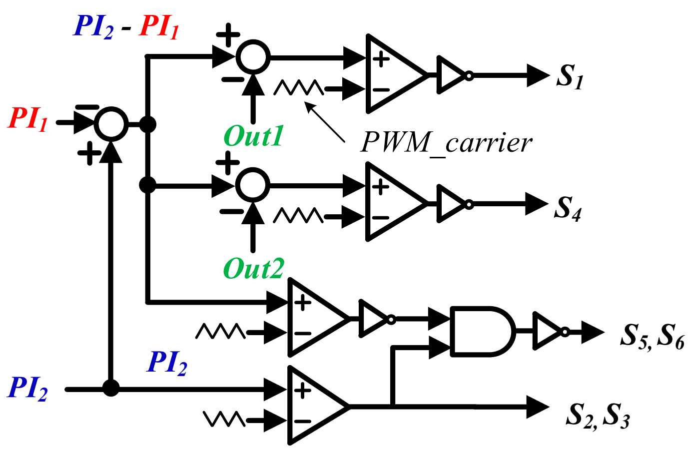

Figure 10. The modulation method of case C.

2.3. Modulation Methods of DIDO Converter for Voltage Balancing in BDCMG

The previous balancing methods are implemented with an active input source; i.e., converters supply power from an input source to an unbalanced load of the bipolar bus with balancing control, or balancing control is possible only when power from the input source is supplied to the load. Because the combined converters simultaneously perform balancing and power control with modulation, the voltage balancing operation is limited by the condition of input sources, for example, PV, battery application, and fuel cell. However, as BDCMG always maintain voltage balancing, an additional balancing method is required. Therefore, the DIDO converter circuit has buck-boost-based voltage balancer for only voltage balancer mode. The only voltage balancer mode implements the voltage balancer and modulation method, such as a buck-boost converter, as shown in Figure 11. As shown in Figure 12, if the switches (S_1, S_2, S_5 or S_3, S_4 and S_6) are turned on simultaneously, the voltage is only supplied to L_3. The voltage gain in only voltage balancer mode is expressed as follows:

$$\frac{V_{out2}}{V_{out1}} = \frac{d_3}{(1-d_3)}. \tag{10}$$

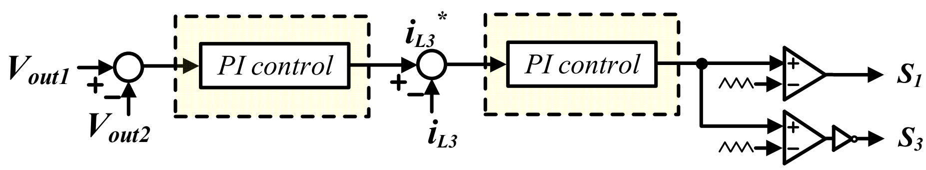

Figure 11. Control block diagram of only voltage balancer mode.

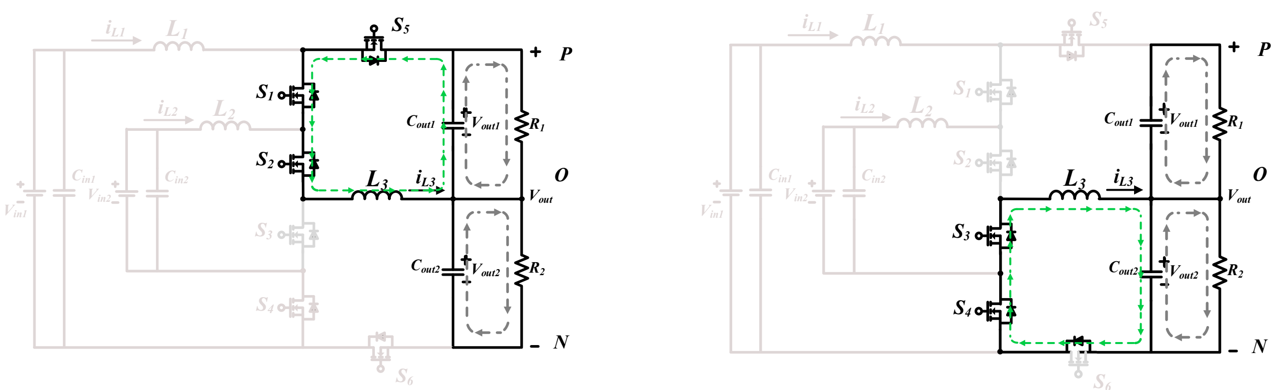

Figure 12. Operating modes of voltage balancer mode without active input sources.

Based on the only voltage balancer mode, the DIDO converter always performs balancing control without active input sources in BDCMG. This mode also controls voltage balancing regardless of the unbalanced power.

2.4. Modeling of DIDO Converter

This converter has independent control loops based on d_1, d_2 and d_3. Control operations based on two boost converters and one buck-boost converter are performed. Based on each operation mode, the small-signal model can be calculated.

$$\frac{\hat{i}_{L_1}}{\hat{d}_1} = \frac{V_{PN}(C_{out1}+C_{out2})s + \frac{V_{PN}}{(R_1+R_2)} + (1-D_1)I_{L1}}{L_1(C_{out1}+C_{out2})s^2 + (\frac{L_1}{(R_1+R_2)} + R_{L_1}(C_{out1}+C_{out2}))s + \frac{R_{L_1}}{(R_1+R_2)} + (1-D_1)^2}. \quad (11)$$

$$\frac{\hat{i}_{L_2}}{\hat{d}_2} = \frac{V_{PN}(C_{out1}+C_{out2})s + \frac{V_{PN}}{(R_1+R_2)} + (1-D_2)I_{L_2}}{L_2(C_{out1}+C_{out2})s^2 + (\frac{L_2}{(R_1+R_2)} + R_{L_2}(C_{out1}+C_{out2}))s + \frac{R_{L_2}}{(R_1+R_2)} + (1-D_2)^2}. \quad (12)$$

$$\frac{\hat{v}_{on}}{\hat{d}_3} = \frac{V_{PO}[\frac{D_3L_3}{R_2}s - (1-D_3)^2]}{(1-D_3)^2[L_3(C_{out2})s^2 + \frac{L_3}{R_2}s + (1-D_3)^2]}. \quad (13)$$

Based on small-signal model, the PI controllers are designed within the stable region. The parameters of the PI controller are as follows: K_{p1} and K_{p2} are 0.3, K_{i1} and K_{i2} are 30, K_{p3} is 3 and K_{i3} is 10.

3. Experimental Results

The experimental results were obtained using a prototype converter to verify the DIDO converter and control methods, as shown in Figure 13. The parameters of the prototype are listed in Table 4. The power switches are used as FCH060N80. In this paper, the control of the DB-BB DIDO converter is implemented using TMS320F28377s.

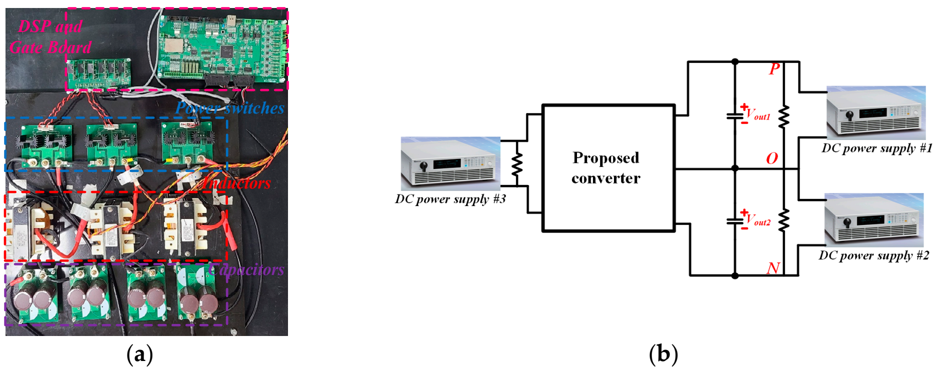

Figure 13. Photograph of prototype converter: (**a**) the prototype; (**b**) configuration of experiments.

Table 4. Parameters of the prototype.

Parameter	Value
Input voltage #1 (V_{in1})	150–170 V
Input voltage #2 (V_{in2})	55–130 V
DC link voltage (V_{out})	190 V
Inductor (L_1, L_2, L_3)	500 µH
Capacitor (C_{in1}, C_{in2}, C_{out1}, C_{out2})	280 µF
Switching frequency (f_s)	20 kHz

3.1. Experimental Result of the DIDO Converter without Voltage Balancing Method

Figure 14 shows the experimental waveforms under an unbalanced load without balancing control, when R_1 and R_2 are 62.3 and 18.7 Ω, respectively. The gate-source voltages of S_1, S_2, and S_5, and inductor current i_{L1} are shown in Figure 14a. In these waveforms, the input voltage conditions are V_{in1} = 150 V and V_{in2} = 130 V and the output current i_{L1} increases when V_{gs1} and V_{gs2} overlap. In Figure 14b, the output voltages V_{out1} and V_{out2} and inductor currents i_{L1} and i_{L2} are shown. The input voltage conditions are V_{in1} = 160 V and V_{in2} = 80 V. V_{out1} and V_{out2} are unbalanced without balancing control and the duty ratios d_1 and d_2 are different depending on the input voltages.

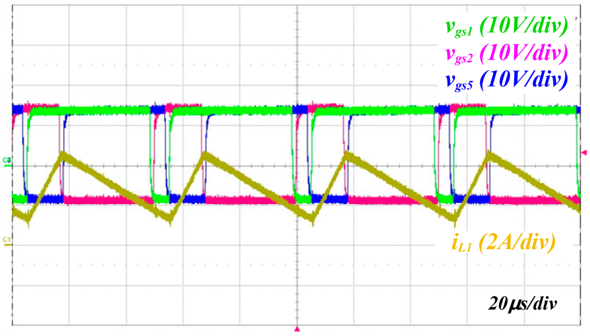

(**a**)

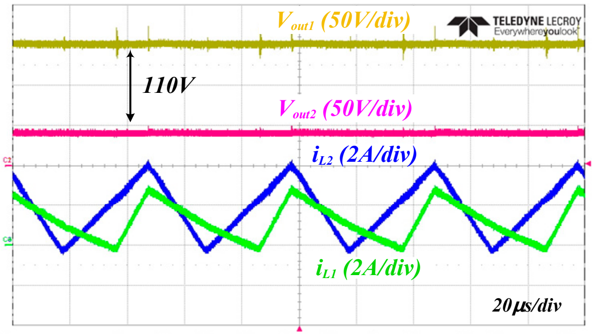

(**b**)

Figure 14. Experimental waveforms of the DIDO converter without voltage the balancing method. (**a**) Gate-source voltages (S_1, S_2, and S_5) and inductor current (i_{L1}). (**b**) Output voltages (V_{out1} and V_{out2}) and inductor currents (i_{L1} and i_{L2}).

3.2. Experimental Results with the Proposed Method in Case A

Figure 15 shows the experimental waveforms of the DIDO converter with balancing modulation in case A. In case A, the switch that implements balancing control uses only S_2. In Figure 15a–c, V_{in1} is 150 V, V_{in2} is 130 V, R_1 is 62.3 Ω, and R_2 is 18.7 Ω. Experimental result of the balancing duty ratio d_3 is approximately 0.5 based on Equation (5), and the inductor current i_{L3} is 3.65 A with unbalanced loads. The gate-source voltages, S_1, S_2, and S_5, and inductor current i_{L3} are shown in Figure 15a. The turn-on time of S_2 is increased by d_3, and S_2 is used for the balancing control because the ON bus is a heavier load than the PO bus. V_{out2}, i_{L1}, i_{L2}, and i_{L3} are shown in Figure 15b; i_{L1} is 1.2 A, i_{L2} is 1.75 A, i_{L3} is 3.65 A and V_{out2} is 95.2 V. As a result, the performance of the modulation method in case A is confirmed under the unbalanced load conditions. Additionally, independent power control and balancing control are performed simultaneously. In Figure 15c, the DIDO converters output a positive output current and simultaneously implement balancing control. The conditions are the same as those in Figure 15b. Likewise, V_{out1} and V_{out2} have a balanced voltage, and the error of the balancing voltage is 0.2 V. In Figure 15d, the boost converters output negative inductor currents and control balancing control; i_{L2} is −1.67 A and i_{L3} is 3.6 A. Based on Figure 15, the proposed modulation and control method of case A are verified with bidirectional and balancing control.

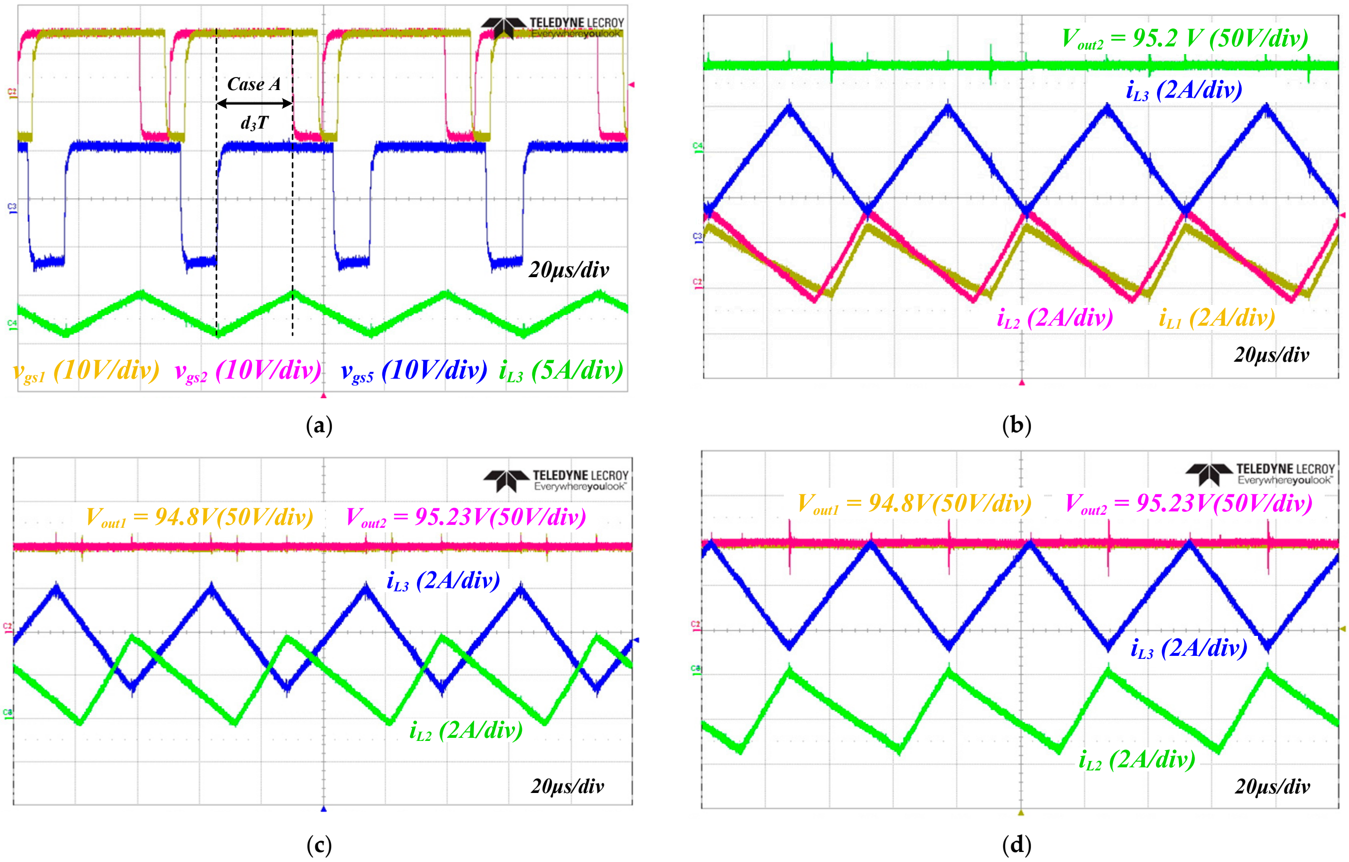

Figure 15. Experimental waveforms of the DIDO converter with balancing control in case A. (**a**) Gate-source voltages (S_1, S_2, and S_5) and inductor current (i_{L3}). (**b**) Output voltage (V_{out2}) and inductor currents (i_{L1}, i_{L2}, and i_{L3}). (**c**) Output voltages (V_{out1} and V_{out2}), and inductor currents (i_{L2} and i_{L3}). (**d**) Output voltages (V_{out1} and V_{out2}) and inductor currents (i_{L2} and i_{L3}).

3.3. Experimental Results with the Proposed Method in Case B

Figure 16 shows the experimental waveforms of the DIDO converter for case B. In case B, the two switches (S_1 and S_2) perform the balancing control. This case reduces the current ripple of i_{L3} without increasing the switching frequency. In Figure 16a,b, the input voltage conditions are V_{in1} = 160 V and V_{in2} = 80 V, with unbalanced load R_1 = 62.3 Ω and R_2 = 37.3 Ω. The balancing duty ratio d_3 is almost 0.25 in the steady state. In the other cases, the maximum current ripple is 4.7 A; however, the proposed control method in case B reduces to 3 A, as shown in Figure 16. As a result, the theoretical balancing current and experimental balancing current of L_3 are similar.

Figure 16a shows the gate-source voltages of S_1, S_2, and S_5 and inductor current i_{L3}. The turn-on times for S_1 and S_2 increase with d_3. In Figure 16b,c, the boost converters implement positive and negative outputs with balancing control. In Figure 16b, i_{L1} is 1.25 A, and i_{L3} is 1 A. In Figure 16c, i_{L2} is −2 A, and i_{L3} is 1 A. Bidirectional control and balancing control are performed independently. The proposed modulation method for case B is experimentally verified.

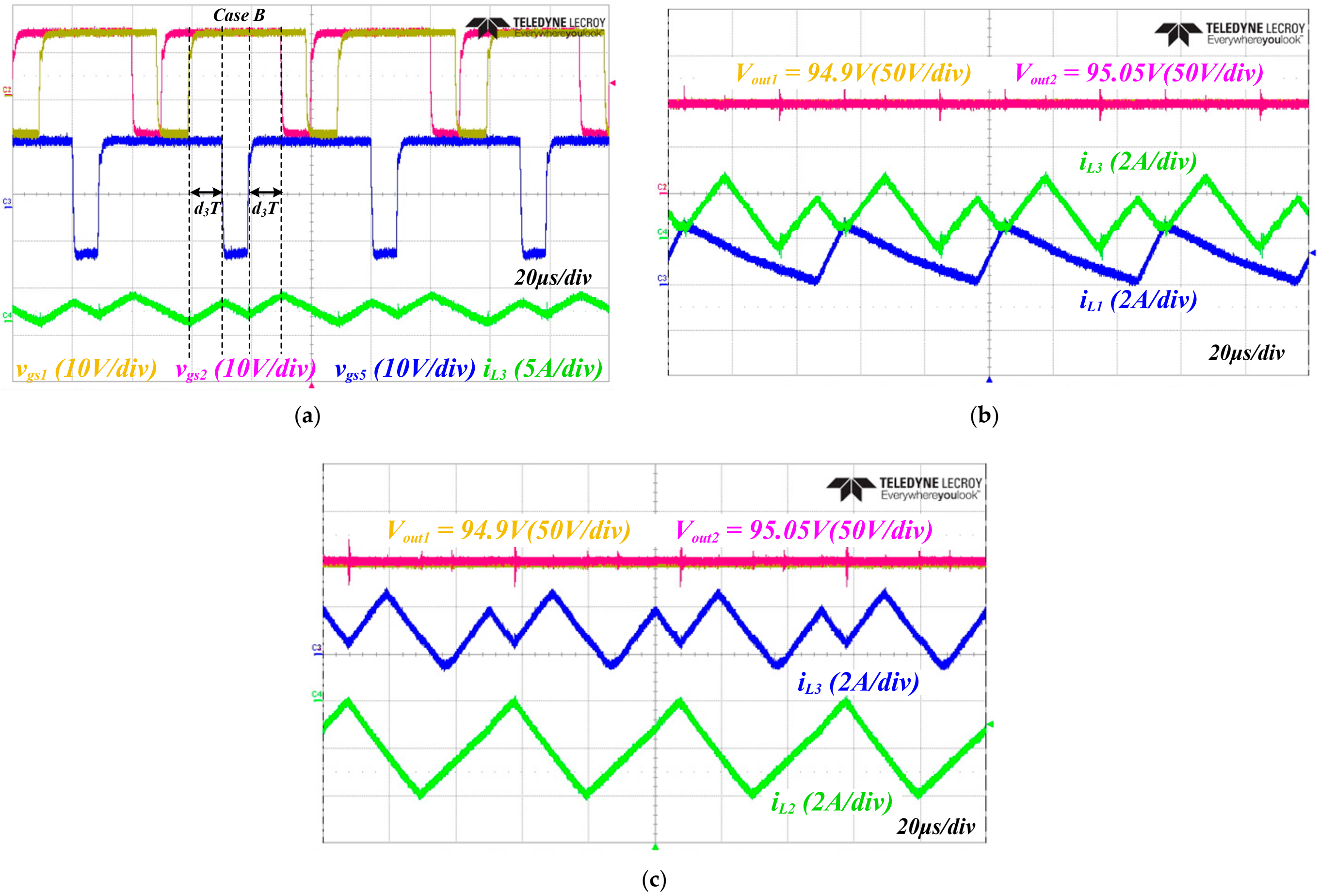

Figure 16. Experimental waveforms of the converter with balancing control in case B. (**a**) Gate-source voltages (S_1, S_2, and S_5) and inductor current (i_{L3}). (**b**) Output voltages (V_{out1} and V_{out2}) and inductor currents (i_{L1} and i_{L3}). (**c**) Output voltages (V_{out1} and V_{out2}) and inductor currents (i_{L2} and i_{L3}).

3.4. Experimental Results with the Proposed Method in Case C

Figure 17 shows the experimental waveforms of the DIDO converter for case C. In case C, only one switch (S_1) performs balancing control. The input voltage conditions are V_{in1} = 170 V and V_{in2} = 55 V. The unbalanced loads are R_1 = 62.3 Ω and R_2 = 18.7 Ω as shown in Figure 17a. In Figure 17a, the turn-on time of S_1 is increased by d_3. The balancing current of L_3 is 3.55 A. The balancing current of L_3 in case C is similar to that of L_3 in case A. In Figure 17b, the unbalanced load R_1 is 31.2 Ω and R_2 is 18.7 Ω. In Figure 17b, the DIDE converters control the negative current with balancing; further, i_{L2} is −1.6 A, and i_{L3} is 2.13 A.

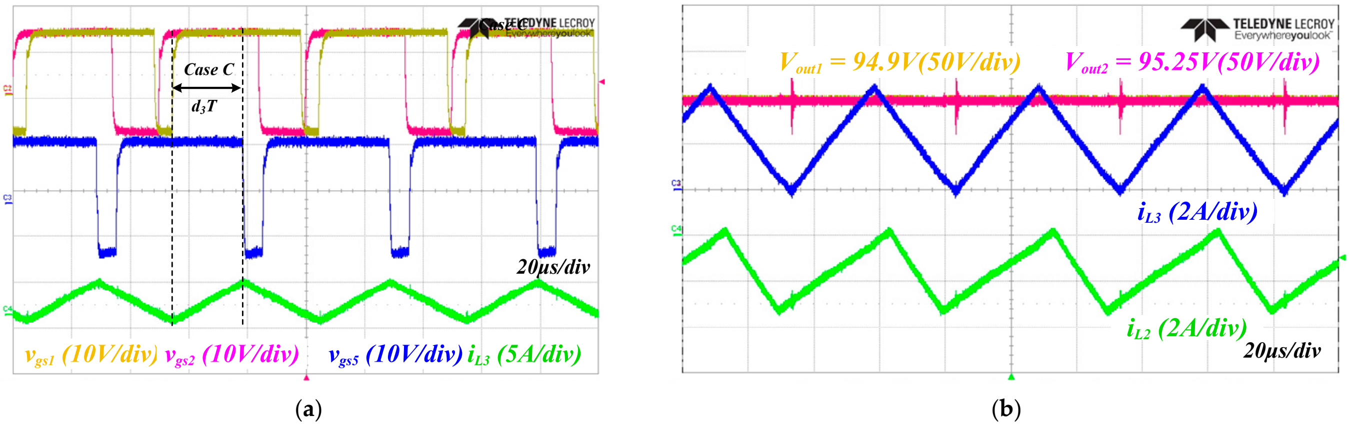

Figure 17. Experimental waveforms of the DIDO converter in case C. (**a**) Gate-source voltages (S_1, S_2 and S_5) and inductor current (i_{L3}). (**b**) Output voltages (V_{out1} and V_{out2}) and inductor currents (i_{L2} and i_{L3}).

3.5. Experimental Result of the Only Voltage Balancer Mode

Figure 18 shows the experimental waveforms of the only voltage balancer mode. The only voltage balancer mode controls V_{out1} and V_{out2} without active input sources. In Figure 18a, R_2 is changed from 37.3 to 18.8 Ω, and V_{out2} is 95 V under the variable unbalanced load with positive balancing currents i_{L3}. Figure 18b shows that the balancing currents i_{L3} is changed from positive to negative under the following changing loads: R_1 changes from 62.4 Ω to 31.2 and R_1 from 18.8 to 37.3 Ω. This mode operates as a voltage balancer without active input sources, but stable voltage balancing is performed.

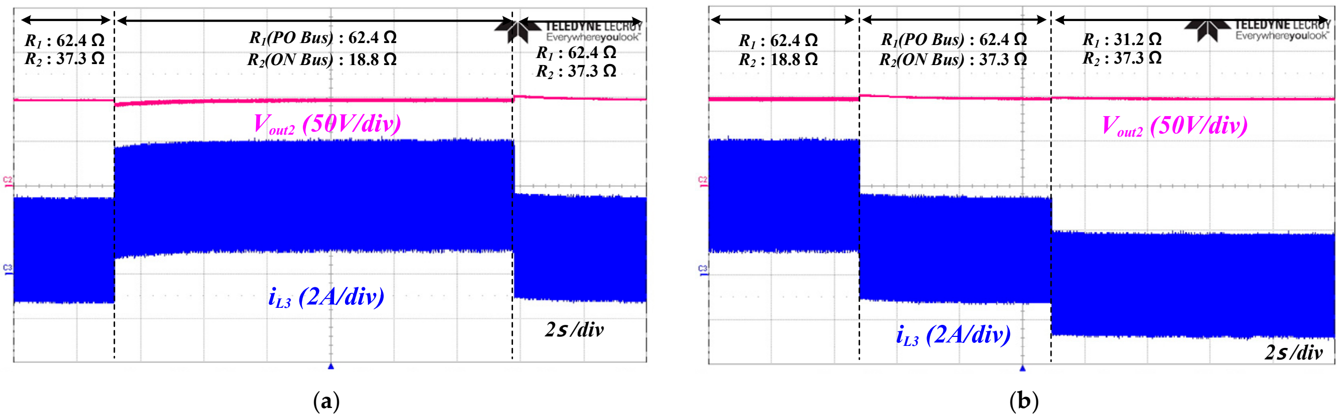

Figure 18. Experimental waveforms of only voltage balancer mode. (**a**) Inductor current (i_{L3}) and output voltage (V_{out2}) for changed load. (**b**) Inductor current (i_{L3}) and output voltage (V_{out2}).

3.6. Comparison of Conventional Converters and the DIDO Converter in BDCMG

Table 5 shows a comparison between the conventional combined converter and DIDO converter for BDCMG. The DIDO converter performs bidirectional control of both input sources and voltage balancing. Balancing control is realized without active input sources, and the DIDO converter controls voltage balancing regardless of the unbalanced power. Therefore, voltage balancing of the DIDO converter is possible under all conditions of a BDCMG. However, voltage balancing of conventional converters is limited, owing to the modulation methods, active input sources, and configuration. Conventional converters perform voltage balancing with an active input source. The proposed control enables voltage balancing even when the input source is not activated. In addition, dual input and voltage balancing control can be controlled independently. Moreover, the converter in [20] controls dual inputs and dual outputs for BDCMG, but it performs unidirectional control. However, the proposed converter controls voltage balancer and dual bidirectional power.

Table 5. Comparison between conventional converter and DIDO converter for voltage balancer in BDCMG.

Topology	No. of Power Switches (MOSFET + Diode)	No. of Inductors + Capacitor (Input and Output)	Power Flow	Controllable Port (Input + Output Source)	Peak Efficiency (Power)
[11]	1 + 2	4 + 5	Unidirectional	1 + 2	88.1% (450 W)
[12]	2 + 2	2 + 3	Unidirectional	1 + 2	89.6% (53.5 W)
[13]	4 + 0	3 + 4	Bidirectional	1 + 2	96.1% (200 W)
[14]	4 + 0	2 + 3	Bidirectional	1 + 2	96.39% (60 kW)
[17]	4 + 2	2 + 3	Bidirectional	1 + 2	-
[20]	2 + 4	1 + 4	Unidirectional	2 + 2	93% (200 W)
This paper	6 + 0	3 + 4	Bidirectional	2 + 2	94.8% (1 kW)

Figure 19 shows the efficiency analysis based on unbalanced loads with WT3000. When the unbalanced power is 760 W and converters #1 and #2 control positive output current, the efficiency of the DIDO converter based on the position of the unbalanced load is analyzed. Under this condition, the ON pole is a heavy load, and the efficiency is high as the current of the switch decreases because i_{L3} is a positive balancing current and i_{L1} and i_{L2} are a positive output current. Furthermore, the PO pole is a heavy load, and the current of the switch increases, because i_{L3} is a negative balancing current. As a result, i_{L1} and i_{L2} are a positive output current.

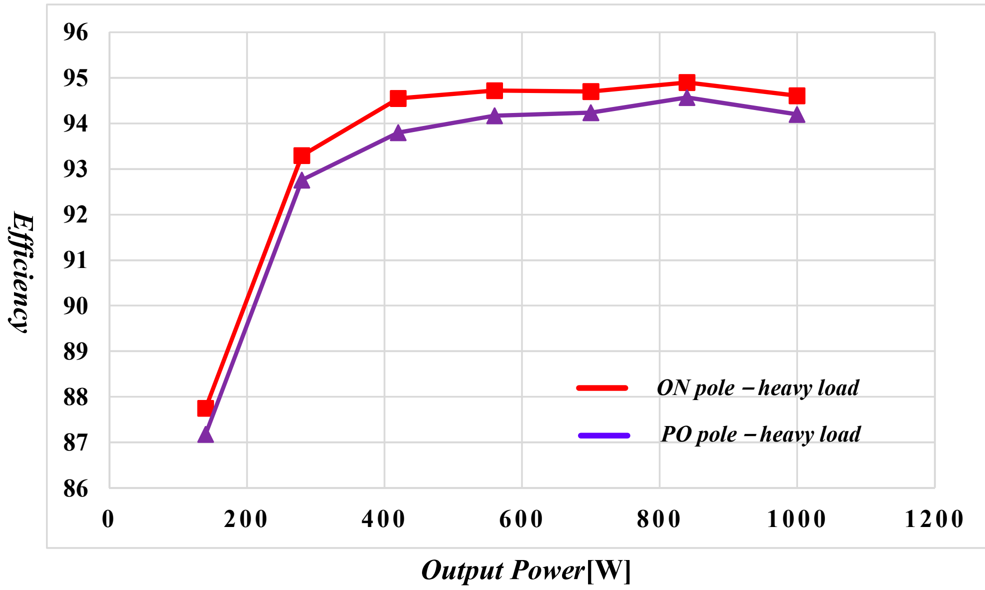

Figure 19. Efficiency analysis based on the unbalanced loads.

Figure 20 shows the performance of voltage balancing for cases A, B and C. The unbalanced load condition is R_1 = 62.3 Ω and R_2 = 18.7 Ω. The Three cases show a voltage deviation of less than 0.5 V. Therefore, it is confirmed that three cases have proper voltage balancing performance.

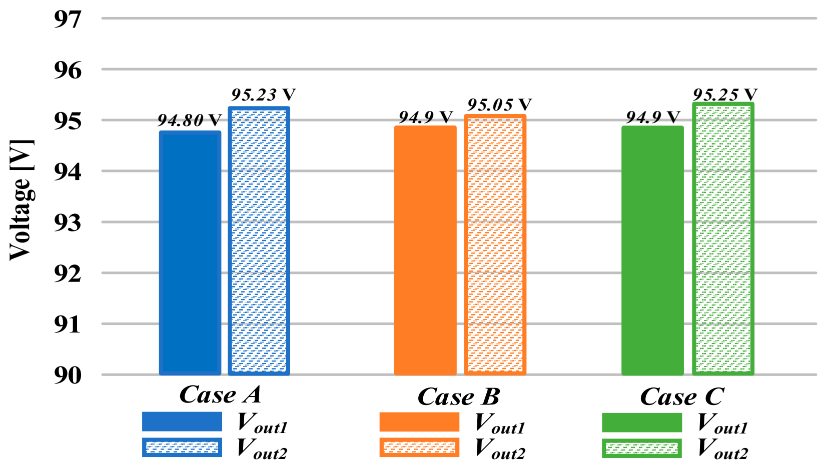

Figure 20. Performance of voltage balancing for cases A, B and C.

4. Conclusions

This paper proposes a bidirectional DIDO converter for voltage balancer in BDCMG. The DIDO converter has two input sources and two output ports connected to the BDCMG, and it simultaneously performs independent bidirectional power control and voltage balancing control. Based on d_1 and d_2, modulation methods are proposed for three cases. Cases A and C have a simple control structure because only one switch is used for the balancing control. In case B, two switches are used for the balancing control, which has a wide operating range, and the current ripple of L_3 is reduced by up to 50% without increasing the switching frequency. The proposed modulations can be used by optimizing for each condition. Since the control loop operates independently, this converter has a simple control structure. Furthermore, only a voltage balancer mode is proposed to perform voltage balancer without an active input source. Voltage balancing is possible by using only two output ports without input sources. As a result, The DIDO converter operates as a voltage balancer under all conditions in BDCMG. Additionally, voltage balancing can be controlled regardless of the unbalanced power. The bidirectional control and voltage balancing performance of the three cases are verified through the experimental results. From the experimental results, the bipolar voltage has a voltage deviation of less than 0.5 V. The bidirectional current control operated stably. Therefore, three cases have proper voltage balancing and bidirectional control performance. As MGs become more popular, this paper will be used in the study of grid-connected converters considering the characteristics of MG.

Author Contributions: S.-H.K. conceived and designed the experiments; S.-H.K. and H.-J.B. performed the experiments; S.-H.K. and H.-J.B. analyzed the data; S.-H.K. and H.-J.B. contributed analysis tools; S.-H.K. wrote the paper. J.Y. and C.-Y.W. participated in research plan development and revised the manuscript. All authors have read and agreed to the published version of the manuscript.

Funding: This research was funded by National Research Foundation of Korea (no. 2019R1A2C2007216).

Data Availability Statement: This study did not report any data.

Acknowledgments: This work was supported by the National Research Foundation of Korea (NRF) grant funded by the Korea government (MSIP; no. 2019R1A2C2007216).

Conflicts of Interest: The authors declare no conflict of interest.

References

1. Wang, P.; Goel, L.; Liu, X.; Choo, F.H. Harmonizing AC and DC: A hybrid AC/DC future grid solution. *IEEE Power Energy Mag.* **2013**, *11*, 76–83. [CrossRef]
2. Dragičević, T.; Lu, X.; Vasquez, J.C.; Guerrero, J.M. DC microgrids—Part II: A review of power architectures, applications, and standardization issues. *IEEE Trans. Power Electron.* **2015**, *31*, 3528–3549. [CrossRef]

3. Guerrero, J.M.; Vasquez, J.C.; Matas, J.; de Vicuna, L.G.; Castilla, M. Hierarchical control of droop-controlled AC and DC microgrids—A general approach toward standardization. *IEEE Trans. Ind. Electron.* **2010**, *58*, 158–172. [CrossRef]
4. Wang, P.; Lu, X.; Yang, X.; Wang, W.; Xu, D. An improved distributed secondary control method for DC microgrids with enhanced dynamic current sharing performance. *IEEE Trans. Power Electron.* **2015**, *31*, 6658–6673. [CrossRef]
5. Lu, X.; Guerrero, J.M.; Sun, K.; Vasquez, J.C. An improved droop control method for dc microgrids based on low bandwidth communication with dc bus voltage restoration and enhanced current sharing accuracy. *IEEE Trans. Power Electron.* **2013**, *29*, 1800–1812. [CrossRef]
6. Kakigano, H.; Miura, Y.; Ise, T. Low-voltage bipolar-type DC microgrid for super high quality distribution. *IEEE Trans. Power Electron.* **2010**, *25*, 3066–3075. [CrossRef]
7. Rodriguez-Diaz, E.; Chen, F.; Vasquez, J.C.; Guerrero, J.M.; Burgos, R.; Boroyevich, D. Voltage-level selection of future two-level LVdc distribution grids: A compromise between grid compatibiliy, safety, and efficiency. *IEEE Electrif. Mag.* **2016**, *4*, 20–28. [CrossRef]
8. Zhang, X.; Gong, C. Dual-buck half-bridge voltage balancer. *IEEE Trans. Ind. Electron.* **2012**, *60*, 3157–3164. [CrossRef]
9. Zhang, X.; Gong, C.; Yao, Z. Three-level DC converter for balancing DC 800-V voltage. *IEEE Trans. Power Electron.* **2014**, *30*, 3499–3507. [CrossRef]
10. Wang, F.; Lei, Z.; Xu, X.; Shu, X. Topology deduction and analysis of voltage balancers for DC microgrid. *IEEE J. Emerg. Sel. Top. Power Electron.* **2016**, *5*, 672–680. [CrossRef]
11. Ferrera, M.B.; Litrán, S.P.; Aranda, E.D.; Márquez, J.M.A. A converter for bipolar DC link based on SEPIC-Cuk combination. *IEEE Trans. Power Electron.* **2015**, *30*, 6483–6487. [CrossRef]
12. Rezayi, S.; Iman-Eini, H.; Hamzeh, M.; Bacha, S.; Farzamkia, S. Dual-output DC/DC boost converter for bipolar DC microgrids. *IET Renew. Power Gener.* **2019**, *13*, 1402–1410. [CrossRef]
13. Prabhakaran, P.; Agarwal, V. Novel boost-SEPIC type interleaved DC–DC converter for mitigation of voltage imbalance in a low-voltage bipolar DC microgrid. *IEEE Trans. Ind. Electron.* **2019**, *67*, 6494–6504. [CrossRef]
14. Kim, S.; Cha, H.; Kim, H. High-efficiency voltage balancer having DC–DC converter function for EV charging station. *IEEE J. Emerg. Sel. Top. Power Electron.* **2019**, *9*, 812–821. [CrossRef]
15. Broeck, G.V.d.; Martinez, W.; Vecchia, M.D.; Ravyts, S.; Driesen, J. Conversion efficiency of the buck three-level DC–DC converter in unbalanced bipolar DC microgrids. *IEEE Trans. Power Electron.* **2020**, *35*, 9306–9319. [CrossRef]
16. van den Broeck, G.; Beerten, J.; Vecchia, M.D.; Ravyts, S.; Driesen, J. Operation of the full-bridge three-level DC–DC converter in unbalanced bipolar DC microgrids. *IET Power Electron.* **2019**, *12*, 2256–2265. [CrossRef]
17. Tavakoli, S.D.; Khajesalehi, J.; Hamzeh, M.; Sheshyekani, K. Decentralised voltage balancing in bipolar dc microgrids equipped with trans-z-source interlinking converter. *IET Renew. Power Gener.* **2016**, *10*, 703–712. [CrossRef]
18. Lee, J.; Cho, Y.; Jung, J. Single-stage voltage balancer with high-frequency isolation for bipolar LVDC distribution system. *IEEE Trans. Ind. Electron.* **2019**, *67*, 3596–3606. [CrossRef]
19. Lee, J.-Y.; Kim, H.-S.; Jung, J.-H. Enhanced dual-active-bridge DC–DC converter for balancing bipolar voltage level of DC distribution system. *IEEE Trans. Ind. Electron.* **2019**, *67*, 10399–10409. [CrossRef]
20. Prabhakaran, P.; Agarwal, V. Novel four-port DC–DC converter for interfacing solar PV–fuel cell hybrid sources with low-voltage bipolar DC microgrids. *IEEE J. Emerg. Sel. Top. Power Electron.* **2018**, *8*, 1330–1340. [CrossRef]